A System for Image Based Finite Element Modeling of Novel Defibrillation Strategies

John K. Triedman, MD
Matthew Jolley, MD
Department of Cardiology
Children's Hospital Boston
300 Longwood Ave., Boston, MA
john.triedman@cardio.chboston.org
matthew.jolley@cardio.chboston.org

Robert MacLeod, PhD
Jeroen Stinstra, PhD
Scientific Computing Institute
University of Utah
50 S Central Campus Dr., Salt Lake City, UT
macleod@cvrti.utah.edu
jeroen@cvrti.utah.edu

Dana Brooks, PhD
Dept of Electrical and Computer Engineering
Northeastern University
360 Huntington Ave., Boston, MA
brooks@ece.neu.edu

Steve Pieper, PhD
Surgical Planning Laboratory
Brigham and Women's Hospital
75 Francis St., Boston, MA
pieper@bwh.harvard.edu

Abstract—Recent development and dissemination of effective and highly automated devices for internal and external defibrillation have impacted the prognosis of sudden cardiac arrest. Evidence for the efficacy and safety and energy dosing of defibrillating devices is based largely on clinical experience in adults, but children and patients with congenital heart disease may have issues of body size and/or cardiac anatomy that may affect the delivery of electric fields to the heart. Finite element modeling may be used in these patients to simulate the effects of standard and novel defibrillation strategies. We present a system designed to allow rapid prototyping of highly-refined finite element models from anatomical images for the study of defibrillation of such patients for the purposes of procedural planning of defibrillation strategies, along with results from exemplary patients. In addition to providing a novel tool for cardiologists caring for these patient groups, this technology will be of significant value to those developing innovative defibrillator designs for patients of more standard body habitus, as well as to those interested in studying the bioelectric properties of the thorax for other applications.

I. INTRODUCTION

The development of digital volume imaging in medicine has created opportunities for patient-specific therapy planning in patients for whom multiple surgical options exists and assumptions of size and/or predictable anatomy are invalid. The utility of such planning has been demonstrated in neuorosurgical, maxillofacial, vascular and orthopedic disciplines. In this project, we extend this approach to predicting the effects of various strategies for cardiac defibrillation in children and in patients with congenital heart disease (CHD), by development of a system for rapid and interactive creation of high-resolution finite element models (FEMs) derived from CT scans of the torso. These models are then used to predict the myocardial electrical fields expected to be generated using differing electrode poses.

Although cardiac defibrillators (ICDs) are designed to work with high reliability in adults, anatomical limitations of body size and cardiac anatomy render standard adult use of ICDs difficult or impossible in pediatric and CHD patients. Out of necessity, various *ad hoc* surgical and technical approaches to implantation have been used to adapt available technology to these special populations [1-3], but only anecdotal reports exist to suggest the safety and efficacy of these techniques. The literature is similarly sparse on optimum paddle placement for external defibrillation, a significant topic given the emergence of public access defibrillation. There are no platforms for defibrillation studies that have the ability to answer these questions or to generate appropriate testable hypotheses. It is our hypothesis that clinically significant variations in defibrillation may exist among the options available to the practitioner, and that knowledge of these difference may be of value in choice of therapy.

Our objective is to develop an open-source software pipeline which will allow the clinician to move rapidly from standard DICOM images of the torso and geometric descriptions of electrodes to treatment planning, using finite element modeling of a variety of clinically feasible approaches to defibrillation in children and other special patient populations. A model is for this pipeline is presented, and initial results defining computationally efficient strategies for FEM specification. Finally, exemplary clinical data from human children relating myocardial field distribution to choice of electrode pose and body size is presented.

II. METHODS

Prior reports demonstrate the validity of the FEM approach in adult torso models of standard defibrillation techniques [4-8]. In these limited models, defibrillation thresholds typically fall within one standard deviation of the mean thresholds reported in clinical studies [9], and are predictive of defibrillation efficacy and efficiency of various intravascular electrode configurations [9-11]. However, clinical use of FEM has been limited by the time and expertise needed to create and manipulate realistic torso and electrode models.

The application pipeline is presented in Figure 1. We have utilized and modified existing, modular open-source software, identified in the Figure [13-15], for segmentation, hierarchical creation of label maps, FEM creation and modeling of myocardial electrical fields.

A. Segmentation and label map generation – Semiautomatic segmentation of 10 tissue compartments is performed using simple thersholding, level sets and statistical techniques [13]. Tissue masks are exported from 3D Slicer as nrrd format datasets, and converted using the UNU toolkit to a composite volume with hierarchical determination of organ assignment made automatically for each voxel. Composite datasets are then imported into BioPSE/SCIRun, and conductivities for these organ domains (extracted from the experimental literature) are assigned to allow modeling of v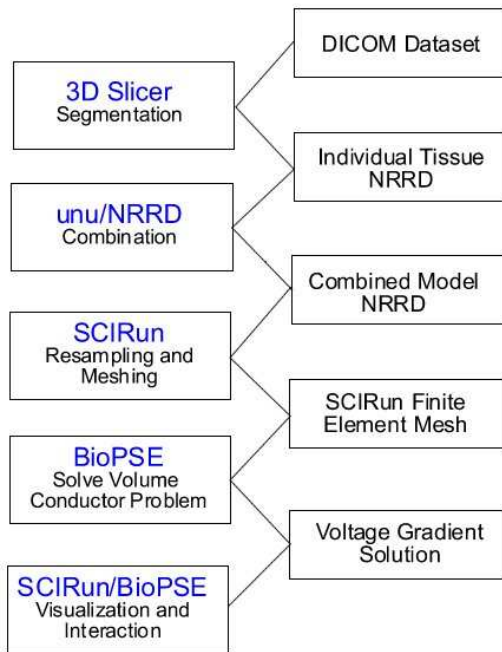oltage fields and current flows [14,15]. A user interface is implemented to allow for interactive, physically realistic modeling of electrode positions.

B. FEM generation – The model is resampled and a mesh is generated using the FEM module with BioPSE/SCIRun. Variable density of hexahedral meshing is used in the vicinity of electrodes to model current density accurately, based on the results of parametric testing of several approaches (see below).

C. FEM solution and data visualization – Voltage values are assigned at specific nodes emulating applied electrode voltages during defibrillation, and the volume conductor problem is solved with subsequent visualization of the resulting voltage gradients within the model (Figure 2). BioPSE/SCIRun modules for automatic modification of the meshed anatomical models to allow repeated interactive relocation of electrodes are in the final testing stages at SCI. The effect of the induced field on the myocardial volume can then be actively interrogated both visually and quantitatively. Evaluation of relative efficiency of the modeled field for defibrillation is performed using the critical mass hypothesis, which suggests that elevation of a high percentage of the myocardial mass to critical voltage threshold reliably results in defibrillation.

Clinical results presented in this report are drawn from more than 300 anatomically distinct electrode poses modeled in 3 torso models in children of varying sizes (12, 32 and 75kg), who had normal thoracic and abdominal CT scans of high quality performed for unrelated clinical indications. Parameter sensitivity analysis of FEM density were performed by comparing solution consistency and standardized computing time for the variety of model-building strategies studied to a fine, completely regular hexahedral mesh grid, taken as the gold standard.

III. RESULTS

A. Clinical studies – Examples of generated data are presented in Figure 2 (next page). The left frame shows the modeled epicardial voltage gradients predicted by the electrode pose modeled, and the right shows the distribution of voltage gradients observed over all myocardial elements as a histogram, with an optimal distribution maximizing the elements shown in green (element $\geq$ 5V/cm) and minimizing those in blue (element <5V/cm) and red (elements $\geq$30V/cm).

Electrode poses are compared in terms of relative efficiency by which they bring an acceptably large fraction of the myocardial mass (chosen to be 95%) to the voltage threshold of 5V/cm by adjusting the applied voltage until this threshold is precisely met. These predicted DFTs can be represented either as the applied voltage or the calculated energy threshold, using the capacitance of the defibrillation system (130 μF) in the equation $E = \frac{1}{2} CV^2$.
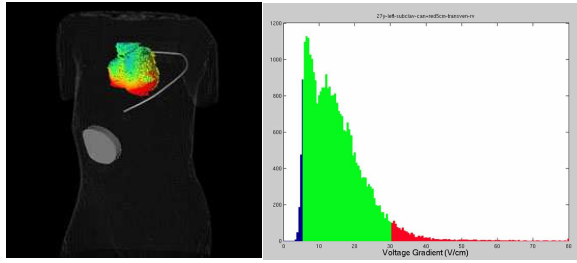

Figure 1. Flow chart of data and the individual tools utilized to create and visual image based finite element models.

Figure 2. Sample model visualization (left frame) shows electrode can positioned in the left upper quadrant of the abdominal wall and a 25-cm electrode positioned subcutaneously in the left 6th thoracic interspace, with voltage gradient magnitude represented in color scale on the epicardial surface. Histogram of voltage gradient in all myocardial voxels (right frame) shows relative fraction of myocardial elements in subthreshold, threshold and injurious ranges of voltage gradient (see text).

Initial model studies show the overall superior efficiency of standard transvenous lead and electrode can placement. However, a variety of alternative poses were nearly equally effective, and depending on body size and the specific geometry proposed, many alternative implant choices fell within the maximum energy which can presently be delivered by some devices. Significant variability of myocardial voltage gradients were seen with relatively small variations of electrode position and body size (Figure 3), and with variations in anode and cathode assignment within a single multielectrode pose. The desirability of contralateral electrode placement when possible was emphasized, and the potential for inducing potentially harmful myocardial voltage gradients by leads in direct contact with the heart was also noted.
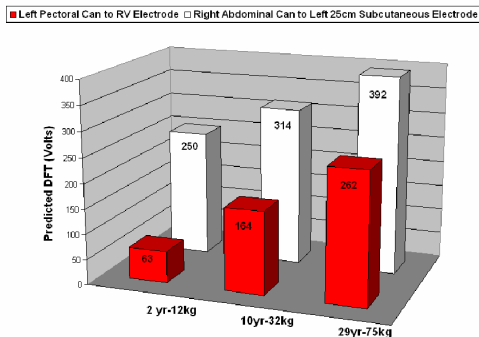

Figure 3. Comparison of defibrillation by body weight of torso models for standard (red) and unconventional (white) electrode poses. Defibrillation voltage meeting threshold criteria varied with size for a given pose, and although this unconventional pose required higher voltage to meet criteria, in the small torso it was less than that necessary for the standard pose.

B. Optimization of FEM design – It was desired to allow for locally high density of FEM in the vicinity of defibrillating electrodes, while maintaining computational efficiency to enhance usability of the modeling system. Strategies tested included reduction in the number of total elements used for FEM construction without local refinement, refinement of the FEM volume in the regions of electrodes and/or myocardium by use of a simple bounding box or local dilation, and adaptive refinement of the FEM in areas determined in preliminary solution to be of high local voltage gradient. Comparison of each technique to a "gold standard" of a fine, regular hexahedral model of 11.3 million elements showed that dilation of elements local to the electrodes only allow reduction in the total number of elements required by 97%, resulting in 92% improvement in computing time and associated with maximum error relative to the standard mesh of ~3% (Table 1).

TABLE 1.

Meshing Method	Max error, $V_{95\%}$	Element number	Relative time
No refinement, grid 75x75x75	16%	4%	5%
No refinement, grid 150x150x150	5%	29%	30%
Bounding box, electrodes	3%	17%	65%
Bounding box, electrodes & heart	2%	19%	162%
Dilation around electrodes	3%	3%	8%
Dilation around electrodes & heart	2%	10%	40%
Adaptive refinement @ 100V/cm	4%	8%	119%
Adaptive refinement @ 150V/cm	6%	8%	27%

IV. FURTHER INVESTIGATIONAL PLANS

A. Algorithms for automatic segmentation of torso anatomy – Certain image processing algorithms have the potential to significantly decrease the time and user oversight currently needed for segmentation of the primary anatomical dataset. Segmented anatomy derived from several typical subjects may be mapped onto the subject data set by warping to determine the most likely patient-specific segmentation [16]. This yields robust results on large organs, but is less effective for structures with considerable intersubject spatial variability (e.g. the vascular tree, which is better treated by level set methods). A further refinement of such automated segmentation has been developed by Pohl [17]. This method combines the strengths of obtained with warping an anatomical atlas, with a statistical classifier to refine the precise localization of object boundaries. Existing segmentation algorithms will be modified to optimize their use in the thorax and abdomen for this application. Given the observed heterogeneity of anatomical structures of interest, it is likely that a structured ensemble of algorithms will ultimately be used for initial, automated segmentation.

B. User defined defibrillation electrode geometries – Widgets are in development to enable structured modification of meshes to represent geometry of defibrillation electrodes,

and to facilitate the interaction of the naïve user with the anatomical model. These support local alterations of the polygonal mesh and model boundary conditions to incorporate the electrodes into the complete simulation model. This will allow accurate more accurate modeling of the interactions of the electrodes with surrounding tissue.

C. Validation studies – Prior studies have established the general validity of the FEM approach for defibrillation modeling in animal and human experimental models [6,8], and by comparison of predicted defibrillation thresholds to clinical values [18]. These studies need to be performed using the current implementation, and in the specific context of extracardiac electrode poses, novel to this project.

V. CONCLUSIONS

Patient-specific bioelectric modeling of the thorax is demonstrated using an integrated, open-source system. Utilization of such systems may be of significant value to clinicians caring for special populations of patients at risk for ventricular fibrillation, by providing predictive information regarding alternative strategies to standard fibrillation prophylaxis or treatment that may be better suited to their unique anatomy. Additionally, this type of software tool is likely to be of direct value to those engaged in development of novel defibrillation devices (e.g., total subcutaneous ICD and other nonstandard techniques [19,20]) for larger populations of normal adults, and those interested in electrocardiographic and cardiac bioelectric research [21, 22].

REFERENCES

1. Berul, C.I., et al., Minimally invasive cardioverter defibrillator implantation for children: an animal model and pediatric case report. Pacing Clin Electrophysiol, 2001 24(12):1789-94.

2. Gasparini, M., Regoli, F., Galimberti, P. and S.G. Priori, Endocardial implantation of a cardioverter defibrillator in early childhood. J Cardiovasc Electrophysiol, 2005. 16(12): p. 1381-3.

3. Stephenson, E.A., et al., A multicenter experience with novel implantable cardioverter defibrillator configurations in the pediatric and congenital heart disease population. J Cardiovasc Electrophysiol, 2006. 17:41-6.

4. DeJongh, A.L., et al., Defibrillation Efficacy of Different Electrode Placements in a Human Thorax Model. PACE, 1999. 22:152-157.

5. Min, X. and R. Mehra, Finite element analysis of defibrillation fields in a human torso model for ventricular defibrillation. Prog Biophys Mol Biol, 1998. 69:353-86.

6. Panescu, D., et al., Optimization of cardiac defibrillation by three-dimensional finite element modeling of the human thorax. IEEE Trans Biomed Eng, 1995. 42:185-92.

7. Wang, Y., et al., Analysis of defibrillation efficacy from myocardial voltage gradients with finite element modeling. IEEE Trans Biomed Eng, 1999. 46:1025-36.

8. Jorgenson, D.B., et al., Computational studies of transthoracic and transvenous defibrillation in a detailed 3-D human thorax model. IEEE Trans Biomed Eng, 1995. 42:172-84.

9. Aguel, F., et al., Impact of transvenous lead position on active-can ICD defibrillation: a computer simulation study. Pacing Clin Electrophysiol, 1999. 22:158-64.

10. Papazov, S., Z. Kostov, and I. Daskalov, Electrical current distribution under transthoracic defibrillation and pacing electrodes. J Med Eng Technol, 2002. 26:22-7.

11. Papazov, S., K. Brandiski, and I. Daskalov, Optimization of the defibrillation current density in the heart region by a two-layer segmented electrode. J Med Eng Technol, 2001. 25:28-33.

12. Yabe, S., et al., Conduction disturbances caused by high current density electric fields. Circ Res, 1990. 66:1190-203.

13. 3D Slicer: Medical Visualization and Processing Environment for Research, http://www.slicer.org, 2004.

14. BioPSE: Problem Solving Environment for modeling, simulation, image processing, and visualization for biomedical computing applications. Scientific Computing and Imaging Institute (SCI), http://software.sci.utah.edu/biopse.html, 2002.

15. SCIRun: A Scientific Computing Problem Solving Environment, Scientific Computing and Imaging Institute (SCI), http://software.sci.utah.edu/scirun.html, 2002.

16. Clatz, O., et al. Robust nonrigid registration to capture brain shift from intraoperative MRI. IEEE Trans Med Imag, 2005 24:1417-27.

17. Pohl, K.M., S. Bouix, R. Kikinis, W. E. L. Grimson. Anatomical guided segmentation with non-stationary tissue class distributions in an expectation-maximization framework. IEEE International Symposium on Biomedical Imaging: Macro to Nano 2004, pp. 81-84, April 2004.

18. Mocanu, D., et al. Patient-specific computational analysis of transvenous defibrillation: a comparison to clinical metrics in humans. Ann Biomed Eng, 2004. 32:775-83.

19. Burke M.C., et al., Defibrillation energy requirements using a left anterior chest cutaneous to subcutaneous shocking vector: implications for a total subcutaneous implantable defibrillator. Heart Rhythm, 2005 2:1332-8.

20. Cesario, D., et al., Azygos vein lead implantation: a novel adjunctive technique for implantable cardioverter defibrillator placement. J Cardiovasc Electrophysiol, 2004 15:780-3.

21. Fischer G. et al. A signal processing pipeline for noninvasive imaging of ventricular preexcitation. Methods Inf Med, 2005 44:508-15

22. Ramanathan C., R.N. Ghanem, P. Jia, K. Ryu, and Y. Rudy. Noninvasive electrocardiographic imaging for cardiac electrophysiology and arrhythmia. Nature Med 2004 10:422-8